Available online at www.sciencedirect.com
SCIENCE DIRECT®

Intermetallics 12 (2004) 741–748

Intermetallics

www.elsevier.com/locate/intermet

# Evaluating abrasive wear of amorphous alloys using nanoscratch technique

A.M. Hodge*, T.G. Nieh

*Lawrence Livermore National Laboratory, PO Box 880, L-350, Livermore, CA 94550, USA*

Available online 21 April 2004

**Abstract**

The hardness and elastic modulus of several Zr, Pd, Cu, and La-based amorphous alloys were investigated using nanoindentation. Abrasive wear of these alloys was also evaluated and compared using nanoscratch techniques under a ramping load. Damage caused by scratching was examined using SEM. Material pile-up took place in all scratched samples, but to different degrees. The scratched surface was observed to be significantly different for alloys with different compositions. A modified Archard equation was derived for the ramping load test. It was found that the wear resistance of amorphous alloys does not follow the classical Archard equation, i.e. the wear resistance is not linearly proportional to the hardness. This discrepancy was suggested to be a result of different wear mechanisms operating in different materials. The wear resistance of a Pd-based alloy was found to be independent of scratch speed.
Published by Elsevier Ltd.

*Keywords:* B. Glasses, metallic; B. Tribological properties; G. Wear-resistant applications

## 1. Introduction

Over the last decade, improvements in the processing quality, quantity and variety of amorphous alloys have led to increased interest in their potential as engineering materials and have increased the need for a full assessment of their mechanical and tribological properties. The latter is of interest since the generally high hardness values of amorphous alloys would make them candidates for high wear applications. However, it has been argued that hardness alone does not determine the wear resistance; in addition to resistance to indentation, crack nucleation and propagation are also responsible for wear [1,2]. Existing results of wear studies often lead to conflicting reports of the wear resistance of amorphous alloys [3–7]. This discrepancy in wear data and its interpretation could be due to oversight of the importance of small differences in processing conditions, which could generate differences in the quality and structure of the alloys. One of the main reasons for the divergence in wear values is the wide variety of acceptable wear tests, which can give significantly different results depending on test conditions such as sliding vs. abrasive wear (two or three body), sliding load and speed, and surface roughness.

Recently, Greer et al. [8] compiled a comprehensive review of the wear properties of amorphous alloys and related materials, mostly Fe and Al-based. However, the large variety of test methods used for assessing the tribological properties of the alloys and incomplete wear data made the task of making a direct comparison among these alloys quite challenging. Nevertheless, it was demonstrated that wear properties of metallic glasses strongly depend upon microstructure. For example, the presence of nanocrystals can improve, but sometimes degrade, wear properties, depending on the type of particle, its size and distribution.

The development of new instrumentation such as the XP-NanoIndenter (MTS, Oak Ridge, TN) [9] provides a convenient method to assess the wear properties of materials. For example, Wang et al [10] used nanoscratch techniques to investigate the wear properties of a Zr-based BMG and found that a lower hardness produces a higher friction coefficient and higher wear; thus, a sample with a mixture of amorphous-nanocrystalline structure is more wear resistant. This result was further illustrated by the work performed by Branagan et al. [11] on steel BMGs, in which the authors concluded that the development of nanostructures on the steel BMG significantly increased the hardness and thus the wear resistance.

The purpose of this work is to compare the wear properties of a variety of amorphous alloys under similar

* Corresponding author. Fax: +1-925-422-6892.
*E-mail address:* hodge4@llnl.gov (A.M. Hodge).

0966-9795/$ - see front matter Published by Elsevier Ltd.
doi:10.1016/j.intermet.2004.02.014

testing conditions using an XP-NanoIndenter. The effects of hardness and chemical composition on the overall wear behavior at various loads and various scratch speeds are investigated.

## 2. Experimental procedures

A total of six alloys (compositions are in at%), $Zr_{65}Al_{10}Ni_{10}Cu_{15}$, $Zr_{52.5}Al_{10}Ti_5Ni_{14.6}Cu_{17.9}$, $La_{55}Al_{25}Cu_{10}Ni_5Co_5$, $Pd_{40}Ni_{10}Cu_{30}P_{20}$, $Pd_{40}Ni_{40}P_{20}$, and $Cu_{60}Zr_{20}Hf_{10}Ti_{10}$, were used in the present study. They are denoted as Zr, ZrTi, La, Pd, PdCu, and Cu, respectively. These alloys were fabricated using various techniques.

The Zr alloy was prepared by warm extrusion using glassy powders initially produced by helium gas atomization under dynamic pressure [12]. The ZrTi sample was processed initially by arc melting the pure elements (Zone-refined Zr bars containing 12.3 ppm O and 10 ppm Hf) in a purified Ar atmosphere and then followed by casting in Cu molds [15].

The Pd sample was prepared by heating the appropriate amounts of pure Pd, Ni, and P to 1127 K at a slow heating rate of 1 K/min in an evacuated quartz capsule [13,14]. The cast ingot was remelted with $B_2O_3$ in a quartz tube with an inner diameter of 5 mm and followed by water quenching. The PdCu sample was prepared in a similar fashion to that of ZrTi; namely, arc melting the pure elements in a purified Ar atmosphere and then casting in Cu molds [13].

The Cu sample was fabricated using a suction cast method. Specifically, an ingot with a nominal composition was arc melted in a copper mold with a mixture of appropriate amounts of highly pure (99.9%) Cu, Zr, Hf, and Ti under a Ti-gettered purified Ar atmosphere. The cast ingot was then broken into small parts, remelted, and then vacuum drawn into a water-cooled copper mold. The $La_{55}Al_{25}Cu_{10}Ni_5Co_5$ alloy was prepared from high-purity elements: La (99.9%), Al (99.9%), Ni (99.98%), and Cu (99.999%). The elements were arc melted under a Ti-gettered argon atmosphere. The alloy was cast into the cavity of a copper mold with a dimension of $1 \times 5 \times 30$ mm$^3$ under an argon atmosphere [15].

Specimens of the above six alloys were mechanically polished to a mirror finish for nanoindentation experiments. Alloys were tested using an XP-NanoIndenter equipped with an Accutip™ (MTS, Oak Ridge, TN) Berkovich indenter, which was calibrated using pure aluminum and silica standards**.** The hardness and elastic modulus measurements were conducted in sets of 25 indents, each indent 2 μm deep and 100 μm apart from the next. Scratch tests were conducted at a speed of 100 μm/s over a length of 500 μm on all test samples. There were at least 15 scratches per alloy under ramping loads from 0 to 40 mN. The orientation of indenter was kept the same for all alloys. Additional scratch tests on $Pd_{40}Ni_{10}Cu_{30}P_{20}$ were conducted at speeds of 0.1, 50, 100, 200 and 400 μm/s over a length of 500 μm in order to study rate effect.

## 3. Results and discussion

### *3.1. Elastic modulus, hardness, and coefficient of friction*

A summary of the mechanical data obtained from the six metallic glasses is listed in Table 1. The average elastic modulus ($E$) and hardness ($H$) are shown for these materials upon which more than 30 indents were performed with negligible deviation from the mean values. In general, the measured $E$ and $H$ for the Zr and Pd-based materials agree well with those previously reported [10,16,17]. As shown in Table 1, all metallic glasses show a modulus and hardness of about 110 and 7 GPa, respectively, except the La alloy. Also, a high modulus is usually accompanied with a high hardness, a result that is consistent with that observed in other metallic glass systems [18].

The coefficients of friction as a function of applied normal load (or sliding distance) for four representative alloys, for $Cu_{60}Zr_{20}Hf_{10}Ti_{10}$, $Pd_{40}Ni_{10}Cu_{30}P_{20}$, $La_{55}Al_{25}Cu_{10}Ni_5Co_5$ and $Zr_{52.5}Al_{10}Ti_5Ni_{14.6}Cu_{17.9}$, are shown in Fig. 1. These coeffient of friction (COF) represent, in principle, the friction between the alloys and diamond. They can be viewed as dynamic, rather than static, friction coefficients. The uncertainty of the initial COF, particularly in the low load region, is associated with the settling down of the indenter head. In Fig. 1, after the settling down, COFs are observed to increase with increasing load for all alloys and the rate of increase (the slope of the curve) notably depends upon the materials. This load sensitivity is material-dependent and is the highest for PdCu and the lowest for La; in an ascending order, it is La, Cu, ZrTi, and PdCu alloy. Notably, this increase of COF as a function of normal load does not follow Amonton's law, i.e. COF is independent of the applied normal load [19].

Material pile-up at the end and sides of a scratch is visible in all three samples (Fig. 2). Also, the amount of pile-up increases with sliding distance, which is primarily caused by the increasing load during ramping scratch. To calculate quantitatively the material pile-up, cross-sectional profiles of scratches from the three alloys were measured and they are shown in Fig. 3. The cross-sectional profile was performed by a surface scan (using 50 μN force) perpendicular to the scratch at the halfway point of the maximum load (20 mN load), i.e. at the scratch distance of about 360 μm from the starting point (see Fig. 4). The profiles are symmetrical, as expected, and appear sharp. It is pointed out in the figure that the scales used for the two axes of the profiles are different. In fact, the ratio of width to depth for the scratch is about eight, which is the same ratio for the shape of the Berkovich indenter. Material pile-up is evident in Fig. 3, especially in the PdCu sample. The heights of

Table 1
Summary of data measured using XP-NanoIndenter

| Composition (at%) | Elastic modulus (GPa) | Hardness (GPa) | Friction coefficient COF | Wear coefficient $K$ | Wear resistance ($10^{11}$ Pa) |
|---|---|---|---|---|---|
| $Zr_{65}Al_{10}Ni_{10}Cu_{15}$ | 101.5 ± 6.7 | 6.8 ± 0.07 | 0.12–0.20 | $2.7 \times 10^{-2}$ | 2.19 |
| $Zr_{52.5}Al_{10}Ti_5Ni_{14.6}Cu_{17.9}$ | 105.0 ± 1.4 | 7.3 ± 0.12 | 0.10–0.17 | $1.4 \times 10^{-2}$ | 5.21 |
| $Pd_{40}Ni_{10}Cu_{30}P_{20}$ | 114.6 ± 4.0 | 6.9 ± 0.08 | 0.15–0.29 | $4.9 \times 10^{-2}$ | 1.73 |
| $Pd_{40}Ni_{40}P_{20}$ | 121.6 ± 1.4 | 6.8 ± 0.07 | 0.15–0.32 | $3.9 \times 10^{-2}$ | 1.36 |
| $Cu_{60}Zr_{20}Hf_{10}Ti_{10}$ | 112.7 ± 1.3 | 7.7 ± 0.10 | 0.10–0.15 | $1.8 \times 10^{-2}$ | 4.28 |
| $La_{55}Al_{25}Cu_{10}Ni_5Co_5$ | 51.6 ± 0.7 | 3.7 ± 0.10 | 0.09–0.16 | $2.3 \times 10^{-2}$ | 1.61 |

pile-up are measured to be 51, 90, and 281 nm, for the Cu, La, and PdCu samples, respectively.

The profiles in Figs. 3 and 4 are consistent; namely, the most damage (i.e. depth of scratch) takes place in PdCu and the least in Cu. It is readily seen in Fig. 3 that the degree of pile-up scales with the depth of scratch. Material pile-up during scratching can affect the COF measurement. When material pile-up occurs, it increases the contact area between the indenter and test sample, thereby causing an increase in the lateral force during sliding. This leads to an apparently higher COF than the actual value. This may be the reason for the observed result of increasing COF with increasing load (Fig. 1) since an increasing load results in an increasing pile-up. This pile-up phenomenon can also be used to explain the observed higher load sensitivity (the slope of the COF-load curve) in the PdCu alloy than that in the Cu and La alloys, since pile-up is more significant in the former alloy.

### 3.2. Abrasive wear

Two methods are usually used to assess wear damage: measurements of the dimensionless wear coefficient, $K$ (or wear resistance coefficient, $R_w$) and visual inspection of wear debris. For two-body wear, a $K$ value ranging from $5 \times 10^{-3}$ to $5 \times 10^{-2}$ is classified as medium/low wear damage [19]. The $K$ values for the present Cu and La alloys ($\sim 1 \times 10^{-2}$) are within this range, suggesting they are reasonable, but not superior wear-resistant materials. By comparison, the PdCu alloy, which shows more wear damage than the La alloy, has a $K$ value of about $5 \times 10^{-2}$, which is near the lower bound of medium/low damage materials.

From Fig. 2, all three alloys show deformation by ploughing, with the PdCu alloy exhibiting the most damage and the Cu alloy the least. (The scratch mark in Cu sample is actually symmetrical, but due to the angle of

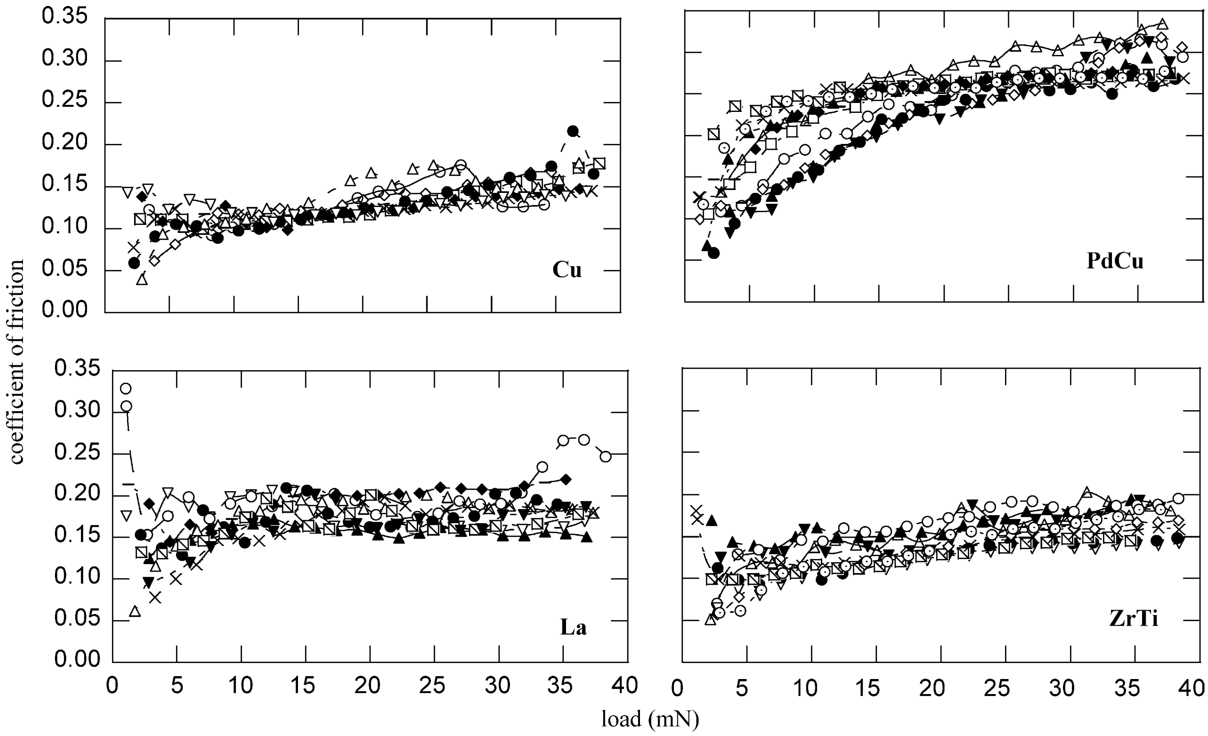


Fig. 1. Friction coefficient plots as a function of load for (a) $Cu_{60}Zr_{20}Hf_{10}Ti_{10}$, (b) $Pd_{40}Ni_{10}Cu_{30}P_{20}$, (c) $La_{55}Al_{25}Cu_{10}Ni_5Co_5$ and (d) $Zr_{52.5}Al_{10}Ti_5Ni_{14.6}Cu_{17.9}$.

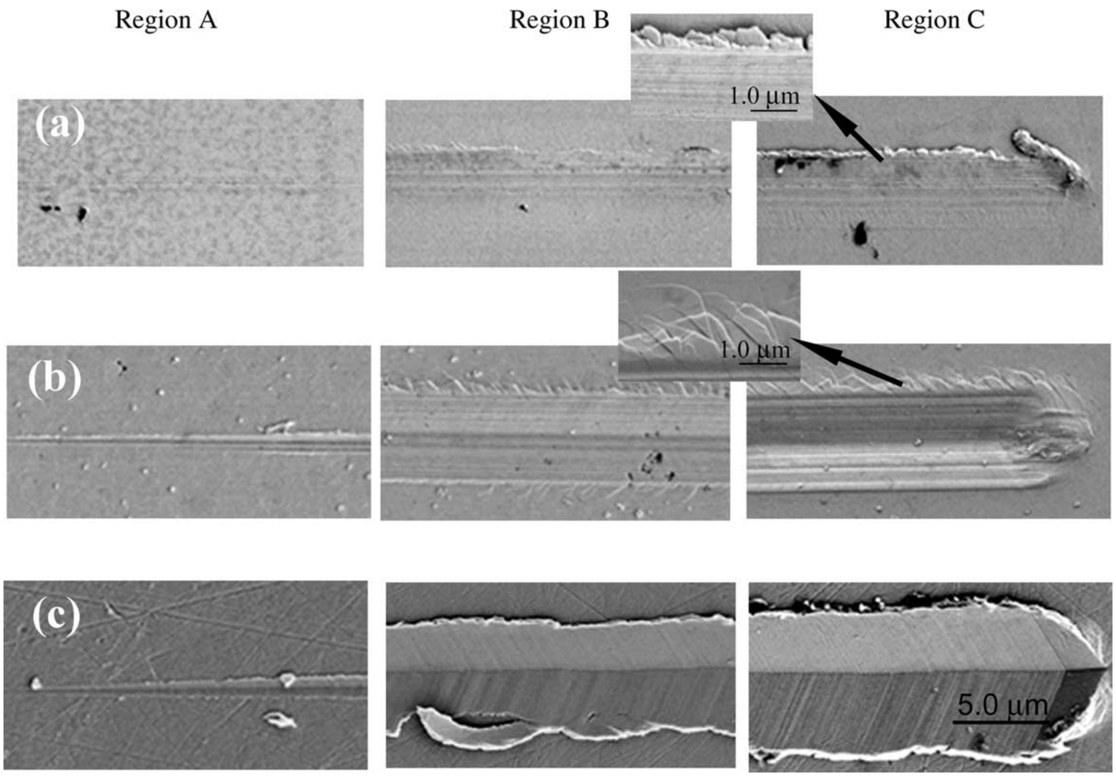


Fig. 2. SEM images of three regions A beginning, B middle and C for end of scratch from three alloys: (a) $Cu_{60}Zr_{20}Hf_{10}Ti_{10}$, (b) $La_{55}Al_{25}Cu_{10}Ni_5Co_5$ and (c) $Pd_{40}Ni_{10}Cu_{30}P_{20}$.

the SEM micrograph, it appears to be non-symmetrical.) The scratched surface on the PdCu alloy exhibits a uniform and clean appearance with a limited amount of debris along the edges and some breakage and pile-up at the end of the scratch. In comparison, the scratch surfaces on the La and Cu samples exhibit a smeared appearance, indicating certain plasticity or interaction between the indenter and testing material. There was practically no debris along the scratch marks. The morphology of the pile-up (or overflowed) material caused by scratching, as revealed in a high magnification inset, appears also different. Shear bands can be readily observed in the La sample, less so in the Cu sample, and are almost nonexistent in the PdCu sample.

Typical scratch depth profiles for Cu, La, and PdCu samples under the same ramping load and scratch distance conditions are depicted in Fig. 4. These three alloys were selected as they represented the highest, intermediate, and lowest hardness materials, respectively. The profiles were calculated as the differential of the pre- and the post-scratch surface profiles (both profiles acquired using a 50 µN load), thus representing permanent plastic deformation. These scratch depth profiles quantitatively correlate well with the cross-sectional profiles shown in Fig. 3. The scratch depth profiles in Fig. 4 are nonlinear in spite of a linear applied ramping load. The final scratch depths for PdCu, La, and Cu are over 300, 270, and 160 nm, respectively. The La alloy, even though its hardness is only about half the value of that of the PdCu alloy, is especially noted to have a material removal that is intermediate.

With the fixed Berkovich indenter geometry, one can readily measure the volume removed from the scratch once the scratch depth and cross sectional profile (Figs. 3 and 4) are known. The volume removed as a function of scratch

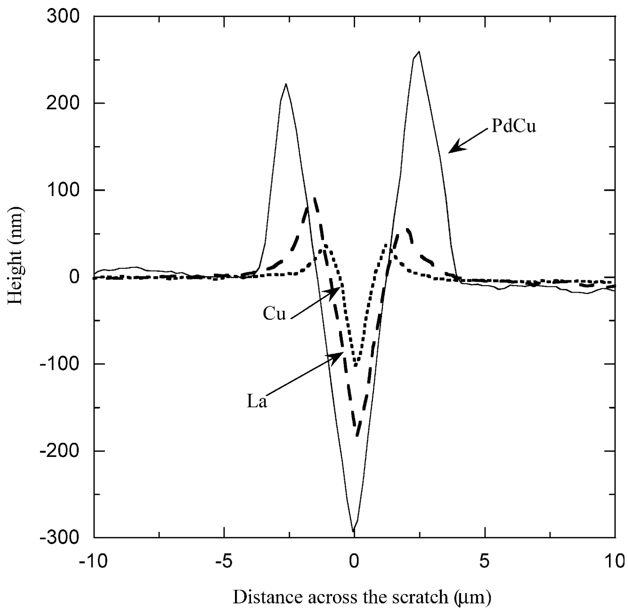


Fig. 3. Cross-section profile of $Cu_{60}Zr_{20}Hf_{10}Ti_{10}$, $La_{55}Al_{25}Ci_{10}Ni_5Co_5$ and $Pd_{40}Ni_{10}Cu_{30}P_{20}$.

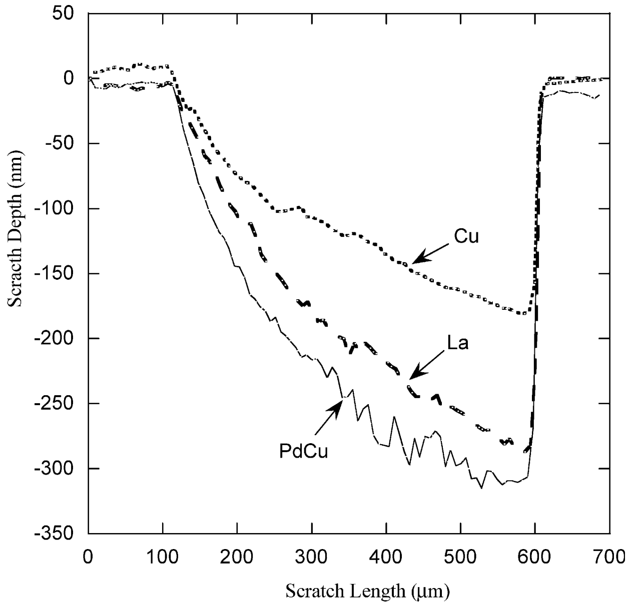


Fig. 4. Scratch depth profile vs. scratch length for $Cu_{60}Zr_{20}Hf_{10}Ti_{10}$, $La_{55}Al_{25}Cu_{10}Ni_5Co_5$ and $Pd_{40}Ni_{10}Cu_{30}P_{20}$.

distance for the six alloys is plotted in Fig. 5. All curves are essentially parabolic in shape. The parabolic shape can be rationalized as follows.

The amount of material removed, d$V$, during scratching over the distance d$x$ is

$$dV = A_s \, dx \tag{1}$$

where, $A_s$ is the sweeping area, that is, the projected area in the direction of scratching. Assuming the hardness is an intrinsic material constant (this is generally true, except for when the indent size is extremely small), the area of

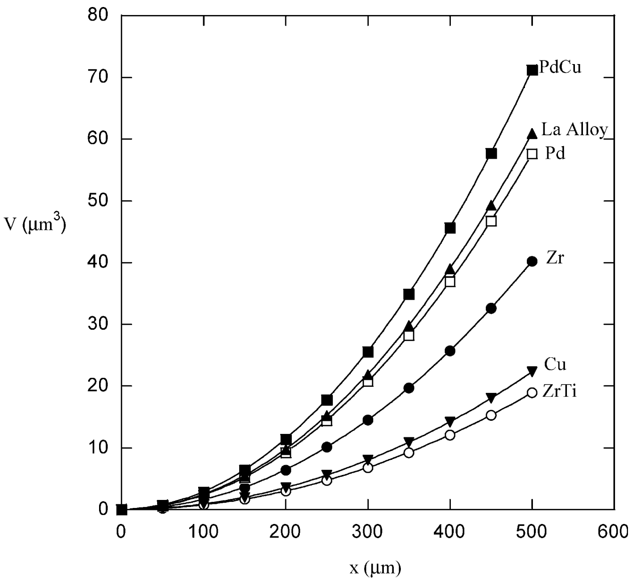


Fig. 5. Volume removed over scratch distance by using Archard wear equation.

projection in the direction of indentation can then be expressed as

$$A_n = \frac{P}{H} \tag{2}$$

where $P$ and H are the applied normal load and hardness, respectively, and $A_n$ is the projected area in the direction of indentation. For the fixed geometry of Berkovich indenter, $A_n$ is linearly proportional to $A_s$, i.e. $A_n = KA_s$. Thus

$$dV = \frac{KP}{H} dx \tag{3}$$

This is essentially the classical Archard equation for sliding wear, where $K$ is the dimensionless wear coefficient [20]. This equation also applies to abrasive wear as discussed elsewhere [19]. In the present scratch tests, the applied ramping load P is proportional to the scratching distance, i.e. $P = Cx$, where $C = 80$ N/m is the proportionality constant. Inserting $P$ into Eq. (3) and performing a simple integration, the volume removed can be written as

$$V = 40K\frac{x^2}{H} \tag{4}$$

This is the modified Archard wear equation [20] for a ramping load. It is indeed in a parabolic form, in agreement with Fig. 5. Once the total volume removal is measured, the dimensionless wear coefficient $K$ can be calculated from Eq. (4), and it is included in Table 1.

According to the modified Archard Equation (Eq. (4)), the harder the material, the less volume removed is expected. However, the present data show that this may not be the case for metallic glasses. As shown in Figs. 3 and 4, the PdCu alloy has a relatively high hardness but has the most material removed and a low wear resistance. By contrast, the La alloy, which has a much lower wear coefficient than the other alloys, has only the second highest volume removed. On the same note, the Cu alloy has the highest hardness and was expected to have the least volume removed, yet the ZrTi alloy actually performed slightly better.

To compare the relative material performance, Fig. 6 shows the correlation between wear resistance and hardness. The wear resistance coefficient $R_w$ is expressed as [21]

$$R_w = \frac{H}{K} \tag{5}$$

where $R_w$ is in the unit of Pa. As shown in the figure, the ZrTi alloy is the most wear resistant alloy, followed by Cu, Zr, PdCu, and finally La and Pd alloy. Since, the La alloy has only about half the hardness of the Pd and Zr-based alloys, it should have been less wear resistant.

The presence of a small amount nanocrystalline phase is known to be able to significantly change the wear resistance of an amorphous alloy [8,10,22]. Thus, a special attempt was made to examine the structure of the amorphous La

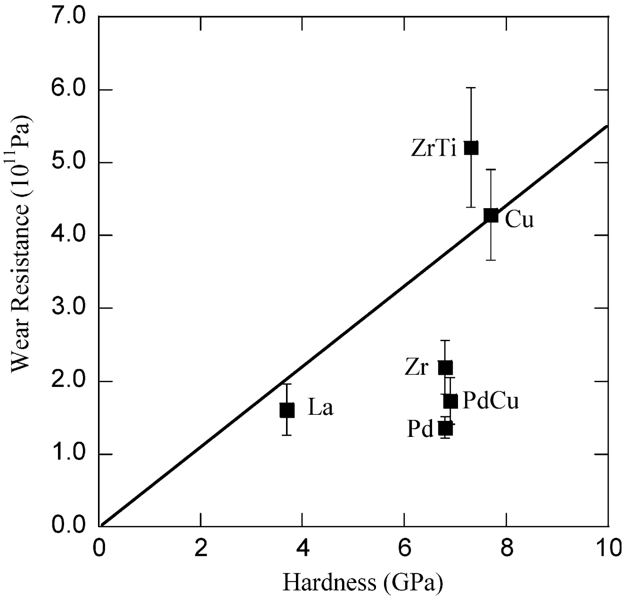


Fig. 6. Comparison of wear resistance vs. hardness for alloy listed in Table 1.

alloy in the present study. An XRD pattern from the alloy (Fig. 7) indicates that it is essentially amorphous. The amorphous nature in the La alloy is also indirectly confirmed by the fact that our measured wear resistance value for the La alloy was consistent with those measured previously from similar La alloys [22]. The above results exclude the possibility that the improved wear resistance in the La alloy is caused by the presence of some nanocrystals.

The resistance of dry wear of a material has been proposed to be determined by a variety of mechanisms as described by Boswell, and Wong and Li [1,2]. In the majority of cases, and especially for brittle materials, the wear resistance is basically determined by the indentation resistance. The wear resistance is therefore proportional to the hardness value (Eq. (5)). However, in some materials,

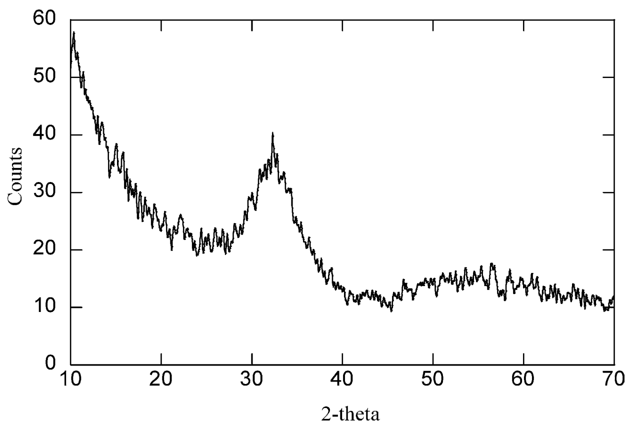


Fig. 7. XRD pattern for $La_{55}Al_{25}Cu_{10}Ni_5Co_5$ (alloy).

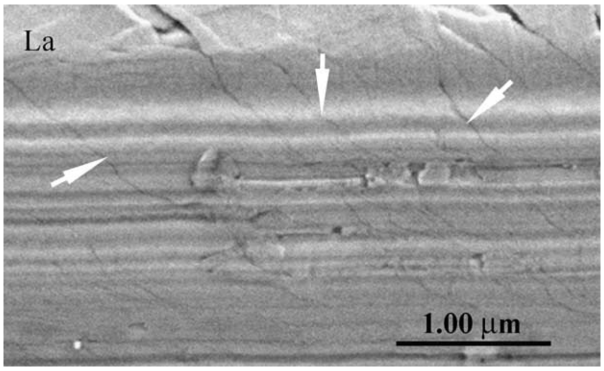


Fig. 8. SEM micrograph of La alloy near the scratch edges.

crack nucleation and propagation are responsible for wear resistance. In this case, wear resistance is not directly related to the hardness. Examinations of the scratched surfaces of the La sample using SEM are shown in Fig. 8, in which fine cracks are readily observed. These cracks are approximately perpendicular to scratch direction. However, because of the dynamic sliding they are slightly tilted. In contrast, no crack was observed on the scratched surface of the PdCu alloy. At the present time, we are unclear about the cause for the morphological difference in the two alloys. Further research is underway.

Another interesting finding from Fig. 7 is the fact that a small substitution of Zr by the addition of Ti, Ni and Cu to the $Zr_{65}Al_{10}Ni_{10}Cu_{15}$ has a significant effect on the hardness and wear resistance. In fact, the Ti-containing alloy has a more than double of hardness and wears resistance. In contrast, the difference between $Pd_{40}Ni_{40}P_{20}$ and $Pd_{40}Ni_{10}Cu_{30}P_{20}$ with a substitution of 30 at% Ni for Cu had a moderate effect on the modulus, but an insignificant effect on the hardness and wear resistance.

### 3.3. Scratch rate effect

To evaluate the rate effect, the scratch depth profiles for PdCu at sliding speeds of 400, 100, 50, 0.1 μm/s are shown in Fig. 9 It is evident that the scratch depth profiles are practically independent of sliding rates, indicating the wear resistance is independent of sliding speed over this range. The independence between wear and sliding speed has also been reported by Imura et al. [5]. Conversely, Wong and Li [2] who studied amorphous $Fe_{81}B_{13.5}Si_{3.5}C_2$ reported that wear rate increased with sliding speed. They attributed the result to structural changes caused by in situ adiabatic heating during sliding. However, it is pointed out that the sliding speed used by them (from 0.005 to 0.5 m/s) is much larger than that used in the present study. Thereby, in situ adiabatic heating is not expected to occur in the present study.

To further evaluate the effect of scratch rate on COF, a comparison of COF as a function of scratch velocity for

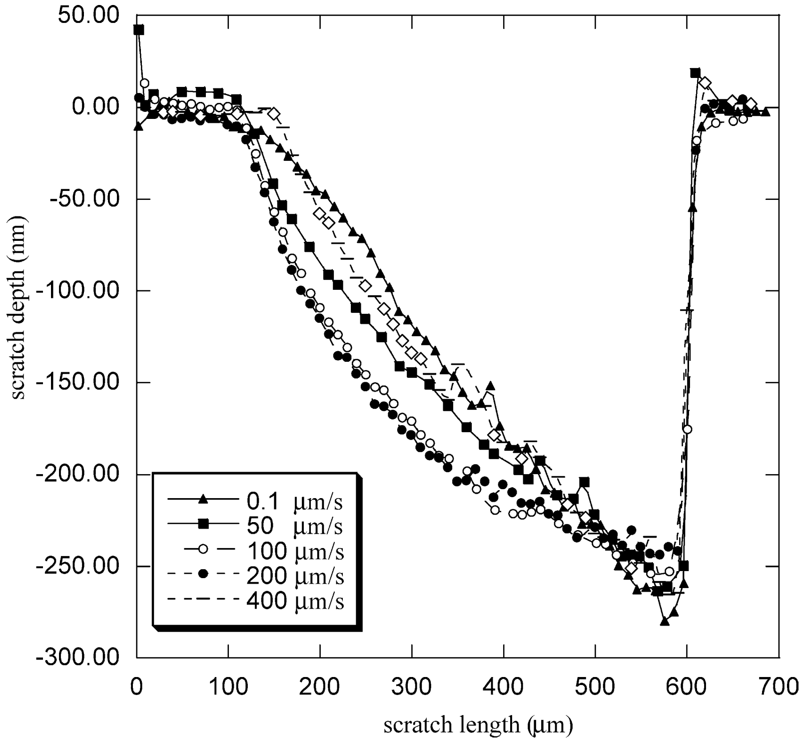


Fig. 9. Correlation of scratch depth and scratch length for $Pd_{40}Ni_{10}Cu_{30}P_{20}$ alloy for five different scratch velocities.

PdCu at 400, 100, 50, 0.1 µm/s for three different loads is presented in Fig. 10. The COF is observed to decrease as the scratch velocity increases, except for the peak at 50 µm/s, for any of the applied normal loads. In addition, at a fixed scratch velocity, the COF increases with increasing applied load. These results are believed to be associated with material pile-up during scratching, as discussed earlier.

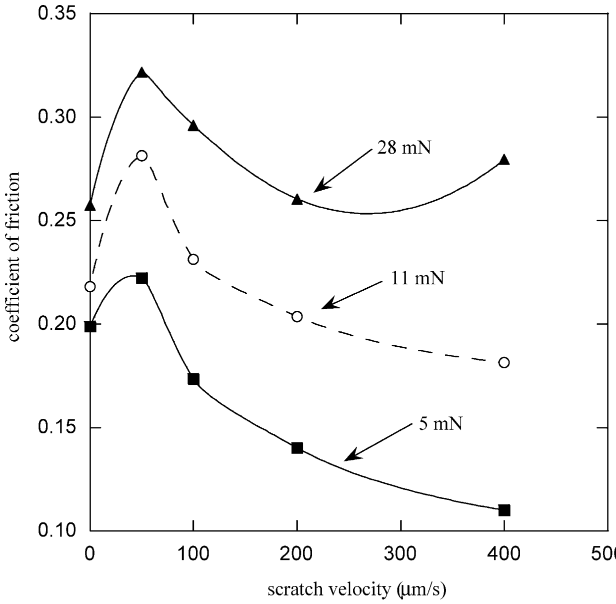


Fig. 10. Coeffient of friction (COF) over scratch velocity at 28, 11 and 5 mN load.

## 4. Conclusion

Six amorphous alloys, $Zr_{65}Al_{10}Ni_{10}Cu_{15}$, $Zr_{52.5}Al_{10}Ti_5Ni_{14.6}Cu_{17.9}$, $Pd_{40}Ni_{10}Cu_{30}P_{20}$, $Pd_{40}Ni_{40}P_{20}$, $Cu_{60}Zr_{20}Hf_{10}Ti_{10}$, and $La_{55}Al_{25}Cu_{10}Ni_5Co_5$, were tested using the XP-nanoindenter to acquire the elastic modulus, hardness and tribological properties. These alloys, except La, show a modulus and hardness of about 110 and 7 GPa, respectively. Their wear resistance, in an ascending order, is $Pd_{40}Ni_{40}P_{20}$, $La_{55}Al_{25}Cu_{10}Ni_5Co_5$, $Pd_{40}Ni_{10}Cu_{30}P_{20}$, $Zr_{65}Al_{10}Ni_{10}Cu_{15}$, $Cu_{60}Zr_{20}Hf_{10}Ti_{10}$, and $Zr_{52.5}Al_{10}Ti_5Ni_{14.6}Cu_{17.9}$. Alloys such as ZrTi and Cu have a reasonable wear resistance, but others such as Pd and PdCu performed rather poorly. Interestingly, the wear resistance of the six amorphous alloys does not follow the classical Archard equation, namely, the wear resistance is linearly proportional to hardness. For example, the $Pd_{40}Ni_{40}P_{20}$ alloy has a hardness value that is twice as much as that for the La alloy, but its wear resistance is poorer than that of La. Morphological examination of scratched surface showed the presence of microcracks in the La sample but not in the Pd sample. This suggests that the above discrepancy may be resulted from different wear mechanisms operating in the two alloys. It was demonstrated that material pile-up during scratching can artificially lead to a higher-than-expected friction coefficient. Scratch velocity appears to have little effect on the wear behavior, at least for the $Pd_{40}Ni_{10}Cu_{30}P_{20}$ alloy.

## Acknowledgements

This work was performed under the auspices of the US department of Energy by the University of California, Lawrence Livermore National Laboratory under contract no. W-7405-eng-48. Helpful discussions with Professor Christopher Schuh at MIT are gratefully acknowledged.

## References

[1] Boswell PG. J Mater Sci 1979;14:1505.
[2] Wong CJ, Li JCM. Wear 1984;98:45.
[3] Dolezal N, Hausch G. Adhesive wear of some (Fe,Ni,Co)—SiB amorphous alloys. In: Steeb S, Warlimont H, editors. Proceedings of the Fifth International Conference on Rapidly Quenched Metals. Amsterdam: North-Holland; 1985. p. 1767.
[4] Morris DG. A study of the wear behavior of amorphous and crystallised metallic alloys. In: Steeb S, Warlimont H, editors. Proceedings of the Fifth International Conference on Rapidly Quenched Metals. Amsterdam: North-Holland; 1985. p. 1775.
[5] Imura T, et al. Mater Sci Engng 1991;133A:332.
[6] Moreton R, Lancaster JK. J Mater Sci Lett 1985;4:133.
[7] Klinger R, Feller HG. Wear 1983;86:287.
[8] Greer AL, Rutherford KL, Hutchings IM. Inter Mater Rev 2002;47(2): 87.
[9] Li X, Bhushan B. Mater Char 2002;48:11.
[10] Wang JG, et al. J Mater Res 2000;15(4):913.
[11] Branagan DJ, et al. Metall Mater Trans 2001;32A:2615.
[12] Kawamura K, et al. Mater Sci Engng 1996;219A:39.
[13] Kato H, et al. Mater Sci Engng 2001;304-306A:758.
[14] Mukai T, et al. Scr Mater 2002;46:43.
[15] Lu ZP, et al. Mater Sci Engng 2001;304–306A:679.
[16] Inoue A. Mater Sci Engng 2001;304–306A:1.
[17] Johnson WL. J Met 2002;54(3):40.
[18] Davis LA, et al. Scr Mater 1976;10:937.
[19] Hutchings IM. Tribology: friction and wear of engineering materials. Boca Raton: CRC Press; 1992.
[20] Archard JF. J Appl Phys 1953;24(8):981.
[21] Rabinowitz E, Dunn LA, Russel PG. Wear 1961;4:345.
[22] Gloriant T. J Non-Cryst Solids 2003;316:96.